Single-Crystal-to-Single-Crystal Post-Synthetic Modification of a Metal-Organic Framework via Ozonolysis

Jorge Albalad,[†,#] Heng Xu,[†,#] Felipe Gándara,[‡] Mohamed Haouas,[§] Charlotte Martineau-Corcos,[§,∥] Ruben Mas-Ballesté,[Δ] Sarah A. Barnett,[⊥] Judith Juanhuix,[◊] Inhar Imaz*[,†], and Daniel Maspoch*[,†,O]

[†] Catalan Institute of Nanoscience and Nanotechnology (ICN2), CSIC and The Barcelona Institute of Science and Technology, Campus UAB, Bellaterra, 08193 Barcelona, Spain

[‡] Materials Science Factory, Instituto de Ciencia de Materiales de Madrid (ICMM), Consejo Superior de Investigaciones Científicas (CSIC), Calle Sor Juana Inés de la Cruz, 3, 28049 Madrid, Spain

[§] Institut Lavoisier de Versailles, CNRS, UVSQ, Université Paris-Saclay, 45 Avenue des Etats-Unis, 78035 Versailles Cedex, France

[∥] CNRS, CEMHTI UPR3079, Université d'Orléans, F-45071 Orléans, France

[Δ] Inorganic Chemistry Department, Universidad Autónoma de Madrid, Madrid-28049, Spain

[⊥] Diamond Light Source, Harwell Science and Innovation Campus, Didcot, Oxfordshire OXII ODE, UK

[◊] ALBA Synchrotron, 08290 Cerdanyola del Vallès, Barcelona, Catalonia, Spain

[O] ICREA, Pg. Lluís Companys 23, 08010 Barcelona, Spain

ABSTRACT: We describe solid-gas phase, single-crystal-to-single-crystal, post-synthetic modifications of a Metal-Organic Framework (MOF). Using ozone, we quantitatively transformed the olefin groups of a UiO-66-type MOF into 1,2,4-trioxolane rings, which we then selectively converted into either aldehydes or carboxylic acids.

Metal-Organic Frameworks (MOFs) are crystalline materials that comprise organic linkers and metal ions/clusters. For the past two decades, they have attracted attention for their exceptional porosity and structural diversity.[1] Beyond their inherent crystallinity and porosity, MOFs are an ideal platform for applications that entail incorporation of target chemical functionalities onto their pore walls.[2-4] To date, several methodologies have been developed to introduce different chemical functionalities into pre-assembled MOFs. These include covalent modification of the organic linkers,[5] ligand exchange processes[6] and post-synthetic metalations.[7,8] However, the synthetic conditions of post-synthetic covalent modifications typically require long reaction times and high temperatures that many MOFs cannot sustain; and for those MOFs that can resist such conditions, the yields are only low to moderate. This is partly because the methods are based on solid-liquid phase processes, whereby reaction progress is limited by the diffusion of reagents inside the porous frameworks to reach the target sites, especially for MOFs whose surfaces are already partially tagged, as the surface groups block access to the pores.[9]

Solvent-less reactivity—particularly, solid-gas phase reactivity—is a widely explored approach in metallurgy and polymer science. Indeed, reactive gases (*e.g.* fluorine gas in steel industry) have been used to quantitatively passivate, cleave, or switch the hydrophobic character of diverse materials.[10] However, there is scant precedent on solid-gas phase reactions with MOFs.[11] We reasoned that such an approach could be used to overcome the aforementioned limitations in post-synthetic functionalization of MOF pores. Here, we demonstrate this concept by reporting transformation of the olefin groups of a UiO-66-type MOF into 1,2,4-trioxolane rings, which we then selectively converted into either aldehydes or carboxylic acids.

Ozone has proven to be a powerful oxidizing reagent for diverse chemistries under mild conditions.[12,13] Of these reactions, ozonolysis of alkenes is arguably the most widely studied.[14,15] Initially used for routine characterization of lipids and natural polymers, it is now employed for selective cleavage of olefinic bonds, as it enables regio-specific formation of aldehydes, ketones or carboxylic acids in mere minutes. This reaction involves the metastable intermediate 1,2,4-trioxolane. Due to their low stability, trioxolane rings are not easy to isolate; however, those that have been are strong antibacterial and therapeutic agents, especially in the form of ozonated oils or triglycerides. Moreover, trioxolane rings can be treated under mild reductive or oxidative conditions to form aldehyde moieties[16] or carboxylic acids,[12] respectively.

Here, we report post-synthetic functionalization of the porous olefin-tagged UiO-66-type MOF, **ZrEBDC**, using controlled, solid-gas phase ozonolysis. We selected it because MOFs of this type exhibit high thermal and chemical stability and are resistant to aqueous and acidic conditions. Additionally, we chose 2-ethenylbenzene-2,4-dicarboxylic

acid (H_2EBDC) as the organic ligand because it is a simple and robust linker with no reactive sites other than its olefin-tagged pendant arm (Figure 1a). We demonstrate that, by constantly streaming ozone through **ZrEBDC**, the pendant alkene groups can be quantitatively transformed into stable 1,2,4-trioxolane moieties on the pore walls, with no loss of single-crystallinity. Moreover, optimized work-up conditions enabled cleavage of these 1,2,4-trioxolane rings to selectively form aldehydes or carboxylic acids (Figure 1a).

Bulk **ZrEBDC** was synthesized by adding an equimolar mixture of H_2EBDC and $ZrOCl_2 \cdot 8H_2O$ into a mixture of DMF and formic acid, and the resulting slurry was then heated at 120 °C. After 12 h, the crude solid was washed twice with DMF and acetone, filtered, and activated under vacuum prior to any ozonolysis test. Colorless octahedral crystals of **ZrEBDC** suitable for Single-Crystal X-Ray Diffraction (SCXRD) were obtained by dissolving the two reagents in a 3:1 mixture of DEF/formic acid, and then heating the resulting solution from 25 to 135 °C (heating rate = 5 °C/min) for 72 h (Figure S2). The crystal structure of **ZrEBDC** revealed the formation of the archetypical UiO-66-like backbone, in which the olefinic side-chains of the EBDC linkers point inwards towards the pores (Figures S3,S4).

In a typical ozonolysis experiment, activated **ZrEBDC** (50 mg) was packed inside a 3.4 mm diameter Pyrex tube (Figure 1b, Figure S1). Two cotton stoppers were added around the sample, and the tube was bent into a U-shape using a flame torch. One end was directly attached to an ozone generator, whereas the other was connected to vacuum. Before the reaction was started, the tube was immersed into a dry-ice/acetone bath at −78 °C and purged under vacuum for 10 min. Under these conditions, ozone presents a moderate half-life and selectively reacts with unsaturated moieties. Excessive generation of ozone was avoided by adding an aqueous KI detector to the end of the setup. Once the sample had reached the proper temperature, a constant stream of O_3/air (10 mmol O_3/h, dried through $CaCl_2$) was blown into the reaction from one end of the tube. The stream was maintained until the KI solution changed from colorless to bright yellow (after ~ 30 min), which indicated that all the olefins had been transformed. The ozone stream was then stopped immediately. The sample, which showed a blue color, was left under vacuum for an additional 10 min to ensure that all the residual unreacted ozone was evacuated from inside the tube; after this, the sample became white again.

We characterized the ozonolyzed crystals (hereafter called **ozo-ZrBDC**) by SCXRD, which confirmed that they had retained the crystallinity and the UiO-66 framework of the starting MOF (Figure 2a). Analysis of the difference Fourier maps revealed high electron-density within the pores of the framework, which we attributed to the 1,2,4-trioxolane. Due to the high symmetry of the framework, the positions of the 1,2,4-trioxolane groups were statistically disordered, which prevented us from refining their position in the cubic *Fm3-m* space group of **ozo-ZrBDC**. Nonetheless, upon refining the framework atoms (including the defect sites and adsorbed species),[17] we calculated a residual electron-density within the pores of 657 e^- per unit cell, using the program Squeeze.[18] This value is in good agreement with the calculated number of electrons corresponding to the presence of one 1,2,4-trioxolane per organic linker within the unit cell (653 e^-), which is the value obtained when 15% of the linker sites are considered to be defective (as suggested by our single-crystal refinement). To determine the orientation of the 1,2,4-trioxolane groups, we performed an additional single-crystal refinement in the monoclinic *C2*-space group. Due to the low partial occupancies of the 1,2,4-trioxolane and their positional disorder, rigid body restraints were employed, whereby the conformation of the 1,2,4-trioxolane moiety was obtained from DFT based calculations. The 1,2,4-trioxolane rings appeared to be rotated relative to the plane of their corresponding linker phenyl ring, and in all cases oriented towards the inorganic SBUs, at short-contact distances (range: 2.3 Å to 3.1 Å) between the 1,2,4-trioxolane atoms and the carboxylic groups of the adjacent linkers, in good agreement with DFT calculations (Figure 2a).

To further confirm the presence of the 1,2,4-trioxolane groups, we compared solid-state ^{13}C NMR spectra, recorded in Cross-Polarization under Magic-Angle Spinning (CPMAS), of the starting **ZrEBDC** and the **ozo-ZrBDC**. The two ^{13}C-peaks of the ethenyl group in **ZrEBDC** appear at 115.6 and 131.0 ppm (Figure 2b, red spectrum). As expected, the spectrum of **ozo-ZrBDC** lacks these two peaks and shows two new ones, at 93.6 and 101.8 ppm (Figure 2b, blue spectrum), which indicated successful conversion of all the olefinic moieties. We then recorded CPMAS-NMR spectra of each product under Polarization Inversion (CPPI),[19] in order to differenciate between carbon sites coupled to protons with contrasted dipolar interaction. In the CPPI spectrum of **ozo-ZrBDC** (Figure 2b, orange spectrum), the resonance at 93.6 ppm is present, whereas that at 101.8 ppm is absent. These observations confirmed the formation of the 1,2,4-trioxalane ring, with the CH_2 peak located at 93.6 ppm and the CH peak, at 101.8 ppm; in agreement with literature data[20] and the solution study shown in the Supporting Information. We further confirmed this formation by performing a soft-ligand exchange experiment (Supporting Information), from which two peaks corresponding to the CH and CH_2 groups of the 1,2,4-trioxolane ring (δ = 5.61 and δ = 4.65 ppm, integrating in a 1:2 ratio) were identified (Figure 2c).

To gain further insight into the ozonolysis reaction, we systematically studied it using various reaction times (5, 10, 15 and 30 min). To this end, the degree of conversion of the olefinic groups into 1,2,4-trioxolane rings was monitored by measuring the ^{1}H NMR spectra of the digested samples (5% HF/DMSO-d_6), and then compared to that of the starting **ZrEBDC** (Section S4). The spectrum of the digested **ZrEBDC** showed the characteristic peaks of three non-equivalent olefinic protons at δ = 7.29, 5.77 and 5.41 ppm, integrating in a 1:1:1 ratio. In contrast, the spectrum of the fully converted **ozo-ZrBDC** confirmed a quantitative fading of these olefinic signals in approximately 30 min of solid-gas interaction. Italso confirmed the formation of four byproducts (two sym-metric trioxolane-metathesis products, 1,2,4-benzenetricarboxylate, and formic acid; Scheme S1) in solu-tion coming from exposing the released 1,2,4-trioxolane-containing linker under aggressive acidic conditions.14 The results at intermediate reaction times confirmed a direct correlation between the disappearance of the olefinic signals and the appearance of the new ones: with conversions of 33% at 5 min; 52% at 10 min; 78% at 15 min; and 100% at 30 min (as previously confirmed by CPMAS-^{13}C NMR).

Samples exposed to different ozonation times were also subjected to standard conditions of MOF-activation (120 °C, 12 h), and their inner surface area was subsequently meas-ured (Figure S25). Compared to the initial SBET value for ZrEBDC (1300 m^2/g; Figure S24), the ozonated samples exhibited decreasingly lower SBET values in function of increasing ozonation time; the value for the fully converted ozo-ZrBDC was 685 m^2/g. Remarkably, this surface area is consistent with a previously reported value for a UiO-66-like MOF with imidazole moieties as pendant groups (SBET = 538 m2/g).[21]

Having demonstrated that ozonide rings can be stabi-lized inside a robust MOF, we next sought to explore the amenability of such rings in ozo-ZrBDC to be selectively reduced into aldehydes or oxidized into carboxylic acids (Figure 1a). For the former, ozo-ZrBDC was soaked over-night, with stirring, in an acidic aq. solution of dimethyl sulfide (Me2S) as reducing agent, to convert the 1,2,4-trioxolane rings into aldehyde groups in a yield of 40% (Fig-ure S20). The mild conditions of the work-up did not allow for quantitative conversion of the stabilized trioxolanes, and all attempts to make the reduction more aggressive resulted in undesired formation of carboxylate byproduct. The SBET of this ozo-ZrBDC partially functionalized with aldehyde moieties was 960 m2/g (Figure S26). Alternatively, soaking ozo-ZrBDC overnight, with stirring, in aq. hydrogen peroxide (H2O2) drove oxidative cleavage of the 1,2,4-trioxolane rings to the corresponding carboxylic acids. This transformation was quantitative, as confirmed by 1H NMR analysis (Figure S21). In both the aldehyde and carboxylic acid products, the UiO-66 type framework was preserved, as confirmed by powder XRD (Figure S23). Furthermore, SCXRD analysis of the crystals resulting from the aggressive oxidation confirmed that they also retained their single-crystal character. Remarkably, the position of the newly formed carboxylic acid groups could be determined through the refinement of the SCXRD data (Figure 3). In this case, the SBET was found to be 301 m2/g (Figure S27), which is in good agreement with those reported for this UiO-66-COOH (SBET = 350-400 m2/g).[22]

In summary, we have reported a solvent-less, solid-gas, single-crystal to single-crystal, post-synthetic functionaliza-tion of a MOF using ozone. Streaming of ozone gas through an olefin-tagged UiO-66-type MOF at -78 °C provided quan-titative transformation of the olefins into 1,2,4-trioxolane rings inside the robust MOF framework. When confined inside the MOF pores, this ring proved to be stable under standard heat and vacuum conditions for MOF activation, unlike in solution. Finally, an optimized work-up enabled further single-crystal to single-crystal chemistry on these 1,2,4-trioxolane rings: reduction into the corresponding aldehyde or oxidation to the corresponding carboxylic acids, the latter in quantitative yield. We are confident that our methodology will offer new insight into how gas molecules might be exploited for MOF chemistry that transcends common physisorption phenomena.

ASSOCIATED CONTENT

Supporting Information

The Supporting Information is available free of charge on the ACS Publications website.

Experimental details, NMR spectra and crystal structures (PDF)

AUTHOR INFORMATION

Corresponding Author

*inhar.imaz@icn2.cat; daniel.maspoch@icn2.cat

ORCID

Inhar Imaz: 0000-0002-0278-1141

Daniel Maspoch: 0000-0003-1325-9161

Author Contributions

[#] J.A. and H.X. contributed equally.

Notes

The authors declare no competing financial interests.

ACKNOWLEDGMENT

This work was supported by EU-FP7-ERC-Co-615954. ICN2 acknowledges the support of MINECO through the Severo Ochoa Centers of Excellence Program, under Grant SEV-2013-0295.

REFERENCES

(1) (a) Janiak, C. *Dalt. Trans.* **2003**, No. 14, 2781. (b) Kitagawa, S.; Kitaura, R.; Noro, S. *Angew. Chem. Int. Ed.* **2004**, *43*, 2334.

(2) Wang, Z.; Cohen, S. M.; Stern, C. L.; Hupp, J. T.; Li, J.; Uribe-Romo, F. J.; Chae, H. K.; O'Keeffe, M.; Yaghi, O. M.; Chaudret, B.; Fischer, R. A. *Chem. Soc. Rev.* **2009**, *38*, 1315.

(3) Burrows, A. D.; Cohen, S. M. *CrystEngComm* **2012**, *14*, 4095.

(4) Cohen, S. M. *Chem. Rev.* **2012**, *112*, 970.

(5) (a) Morris, W.; Doonan, C. J.; Furukawa, H.; Banerjee, R.; Yaghi, O. M. *J. Am. Chem. Soc.* **2008**, *130*, 12626. (b) Kim,

M.; Cahill, J. F.; Prather, K. A.; Cohen, S. M. *Chem. Commun.* **2011**, *47*, 7629. (c) Morris, W.; Doonan, C. J.; Yaghi, O. M. *Inorg. Chem.* **2011**, *50*, 6853. (d) Luan, Y.; Qi, Y.; Gao, H.; Andriamitantsoa, R. S.; Zheng, N.; Wang, G.; Čejka, J.; Valenzano, L.; Lamberti, C.; Lillerud, K. P.; Bordigaa, S. *J. Mater. Chem. A* **2015**, *3*, 17320.
(6) (a) Boissonnault, J. A.; Wong-Foy, A. G.; Matzger, A. J. *J. Am. Chem. Soc.* **2017**, *139*, 14841. (b) Kim, M.; Cahill, J. F.; Su, Y.; Prather, K. A.; Cohen, S. M. *Chem. Sci.* **2012**, *3*, 126. (c) Liu, C.; Zeng, C.; Luo, T.-Y.; Merg, A. D.; Jin, R.; Rosi, N. L. *J. Am. Chem. Soc.* **2016**, *138*, 12045.
(7) Bloch, W. M.; Burgun, A.; Coghlan, C. J.; Lee, R.; Coote, M. L.; Doonan, C. J.; Sumby, C. J. *Nat. Chem.* **2014**, *6*, 906.
(8) Manna, K.; Zhang, T.; Lin, W. *J. Am. Chem. Soc.* **2014**, *136*, 6566.
(9) Wang, Z.; Tanabe, K.; Cohen, S. *Chem. - A Eur. J.* **2010**, *16*, 212.
(10) (a) Layer, R. W.; Lattimer, R. P. *Rubber Chem. Technol.* **1990**, *63*, 426. (b) Miki, N.; Maeno, M.; Maruhashi, K.; Nakagawa, Y.; Ohmi, T. *Corros. Sci.* **1990**, *31*, 69. (c) Harshé, G. *J. Mater. Eng. Perform.* **1992**, *1*, 83.
(11) Servalli, M.; Ranocchiari, M.; Van Bokhoven, J. A.; Long, J. R.; Lillerud, K. P.; Tilset, M.; Fischer, R. W.; Fischer, R. A. *Chem. Commun.* **2012**, *48*, 1904.
(12) Cochran, B. *Synlett* **2015**, *27*, 245.
(13) Schiaffo, C. E.; Dussault, P. H. *J. Org. Chem.* **2008**, *73*, 4688.
(14) Criegee, R. *Angew. Chem. Int. Ed.* **1975**, *14*, 745.
(15) Geletneky, C.; Berger, S. *European J. Org. Chem.* **1998**, *1998*, 1625.
(16) Willand-Charnley, R.; Fisher, T. J.; Johnson, B. M.; Dussault, P. H. *Org. Lett.* **2012**, *14*, 2242.
(17) Trickett, C.A.; Gagnon, K. J.; Lee, S.; Gándara, F.; Bürgi, H.-B.; Yaghi, O. M. *Angew. Chem. Int. Ed.* **2015**, *54*, 11162.
(18) Spek, A. L. *Acta Cryst. C*, **2015**, *71*, 9.
(19) Wu, X.; Zlim, K. W. *J. Magn. Reson. Ser. A* **1993**, *102*, 205.
(20) (a) Soriano, N. U.; Migo, V. P.; Matsumura, M. *Chem. Phys. Lipids* **2003**, *126*, 133. (b) Sega, A.; Zanardi, I.; Chiasserini, L.; Gabbrielli, A.; Bocci, V.; Travagli, V. *Chem. Phys. Lipids* **2010**, *163*, 148.
(21) Liang, J.; Chen, R.-P.; Wang, X.-Y.; Liu, T.-T.; Wang, X.-S.; Huang, Y.-B.; Cao, R. *Chem. Sci.* **2017**, *8*, 1570.
(22) Ragon, F.; Campo, B.; Yang, Q.; Martineau, C.; Wiersum, A. D.; Lago, A.; Guillerm, V.; Hemsley, C.; Eubank, J. F.; Vishnuvarthan, M.; Taulelle, F.; Horcajada, P.; Vimont, A.; Llewellyn, P. L.; Daturi, M.; Devautour-Vinot, S.; Maurin, G.; Serre, C.; Devic, T.; Clet, G. *J. Mater. Chem. A* **2015**, *3*, 3294.

Table of Contents

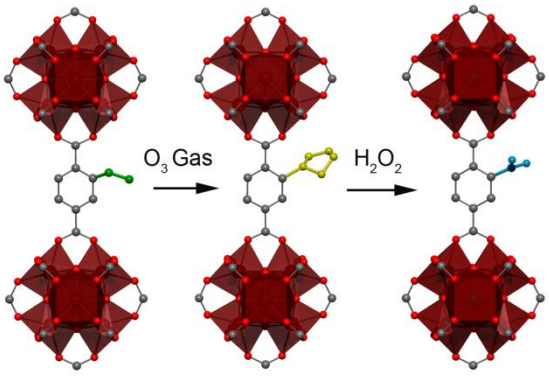

FIGURES

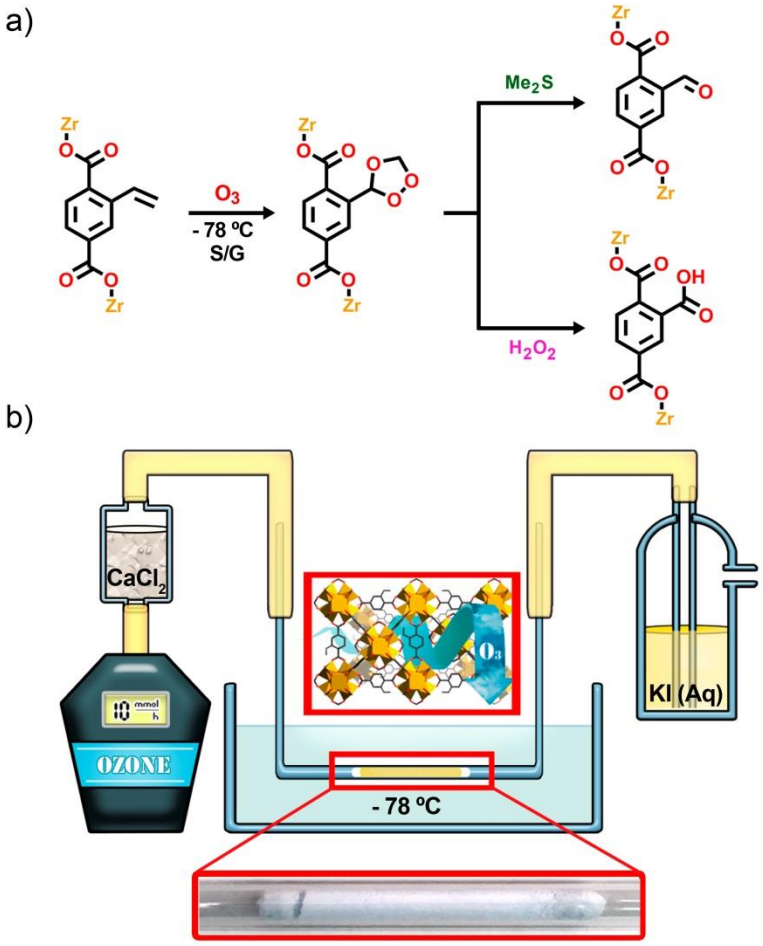

Figure 1. a) Scheme of the post-synthetic modifications performed with ZrEBDC. b) Scheme of the set-up used for the ozonolysis of ZrEBDC. Bottom: photo of the tube containing the crystals.

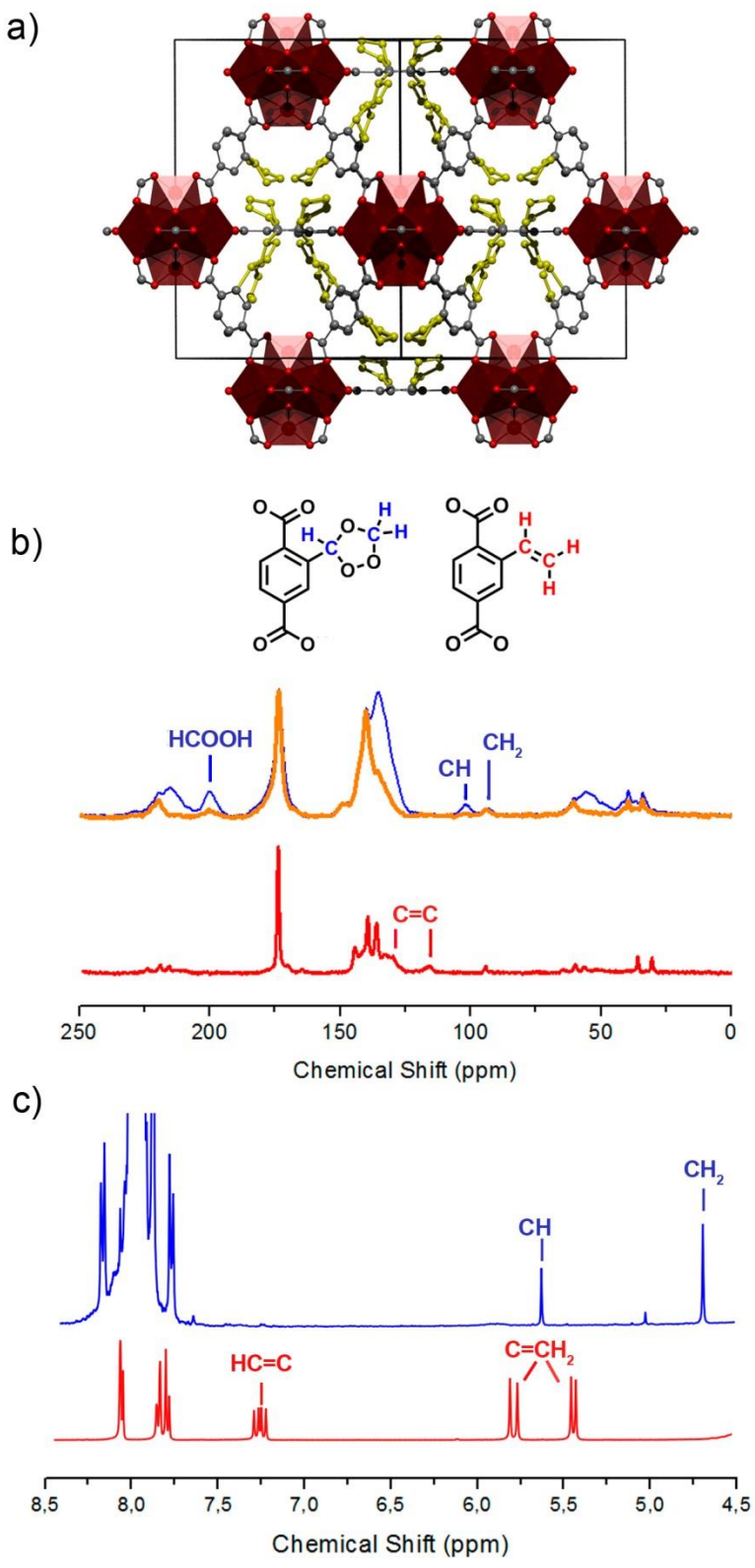

Figure 2. a) Illustration of the single-crystal structure of ozo-ZrBDC across the [110] direction, highlighting the disordered 1,2,4-trioxolane moieties (yellow). b) Solid-state 13C NMR spectra of ZrEBDC (red: CPMAS) and ozo-ZrBDC (blue: CPMAS; orange: CPPI-MAS). c) 1H NMR spectra after the ligand-exchange experiment (blue) and H2EBDC (red).

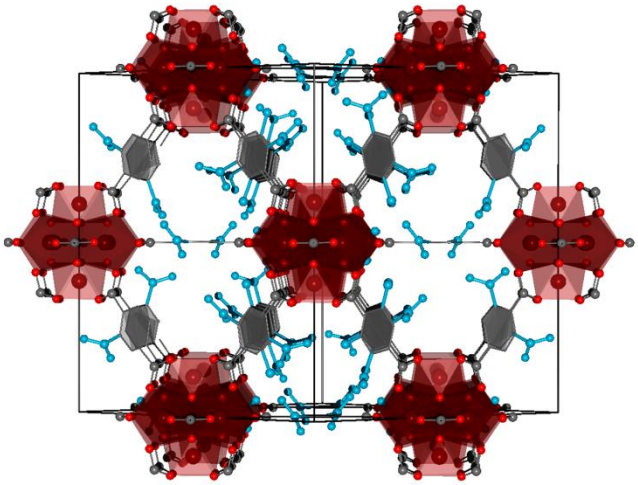

Figure 3. Illustration based on the single-crystal structure of ZrBDC-COOH across the [110] direction, highlighting the disor-dered -COOH moieties (blue).